BIOCHEMISTRY
including biophysical chemistry & molecular biology

Rapid Report

pubs.acs.org/biochemistry

Structures of cGMP-Dependent Protein Kinase (PKG) Iα Leucine Zippers Reveal an Interchain Disulfide Bond Important for Dimer Stability

Liying Qin,[†] Albert S. Reger,[‡,#] Elaine Guo,[§,▽] Matthew P. Yang,[∥,●] Peter Zwart,[⊥] Darren E. Casteel,[@] and Choel Kim*[,†,‡]

[†]Verna and Marrs McLean Department of Biochemistry and Molecular Biology and [‡]Department of Pharmacology, Baylor College of Medicine, Houston, Texas 77030, United States

[§]Department of Chemistry and [∥]Department of Biochemistry, Rice University, Houston, Texas 77005, United States

[⊥]Lawrence Berkeley National Laboratory, Berkeley, California 94720, United States

[@]Department of Medicine, University of California at San Diego, La Jolla, California 92093, United States

Supporting Information

ABSTRACT: cGMP-dependent protein kinase (PKG) Iα is a central regulator of smooth muscle tone and vasorelaxation. The N-terminal leucine zipper (LZ) domain dimerizes and targets PKG Iα by interacting with G-kinase-anchoring proteins. The PKG Iα LZ contains C42 that is known to form a disulfide bond upon oxidation and to activate PKG Iα. To understand the molecular details of the PKG Iα LZ and C42−C42′ disulfide bond, we determined crystal structures of the PKG Iα wild-type (WT) LZ and C42L LZ. Our data demonstrate that the C42−C42′ disulfide bond dramatically stabilizes PKG Iα and that the C42L mutant mimics the oxidized WT LZ structurally.

Cyclic GMP-dependent protein kinase (PKG) (EC 2.7.11.12) is a serine/threonine kinase that regulates smooth muscle tone, vasorelaxation, erectile function, platelet aggregation, circadian rhythm, and gastrointestinal secretion.[1−5] Two types of PKG exist in mammals, soluble PKG I and membrane-bound PKG II, encoded by two separate genes, *prkg1* and *prkg2*, respectively. They are comprised of an N-terminal regulatory domain (R-domain) and a C-terminal catalytic domain (C-domain). The R-domain includes a leucine zipper (LZ) domain, followed by an autoinhibitory (AI) sequence and two tandem cyclic nucleotide binding domains (cNBDs) (Figure 1A). *prkg1* undergoes alternative splicing, giving rise to two isotypes of PKG I, PKG Iα and PKG Iβ, which differ only in the N-terminal ∼100 amino acids, including the LZ domain and the AI sequence, with a degree of similarity of ∼36%.[6,7]

The LZ domain mediates homodimerization and cellular targeting of PKG. The targeting of PKG involves the variable LZ domain binding to a class of anchoring proteins [G-kinase-anchoring protein (GKAP)] in an isotype-specific manner. PKG Iα-specific GKAP includes a regulatory subunit/myosin binding subunit of myosin light chain phosphatase (MYPT1 or MBS)[8−10] and regulator of G-protein signaling-2 (RGS-2).[11] The interaction between PKG Iα and its GKAP is critical for its function in vivo. For example, disrupting the dimerization of the PKG Iα LZ domain abrogates the interaction of the kinase with MYPT1[9,12] and decreases the level of RhoA phosphorylation at Ser188, resulting in higher RhoA activity in mice vascular smooth muscle cells and hypertensive mice.[12] PKG Iα interacts with RGS-2 through the LZ domain, allowing RGS-2 phosphorylation and termination of Gαq-mediated signaling.[11,13] PKG Iβ specifically binds to and phosphorylates inositol 1,4,5-triphosphate receptor I (IP_3RI)-associated PKG substrate (IRAG),[14] decreasing the amount of intracellular calcium release,[15,16] and inhibiting platelet aggregation.[17] As a PKG II-specific interacting protein, Rab11b mediates PKG II trafficking[18,19] and β2-adrenergic receptor recycling.[20] Despite several isotype-specific GKAPs for PKG, little is known about the molecular details underlying GKAP specificity.

Because of the lack of structural information, the current model of PKG activation is largely based on structural studies of its closest homologue, cAMP-dependent protein kinase (PKA), combined with solution studies of PKG.[21] The model suggests that cGMP binding induces conformational changes in which both the axial ratio (length/width) and radius of gyration (R_g) of PKG I increase[22,23] and the catalytic domain is released from the autoinhibitory sequence of the regulatory domain,[24] resulting in kinase activation. Although autophosphorylation increases the basal activity of PKG I,[25,26] binding of cGMP to both cyclic nucleotide binding sites of PKG is required for full activation.[2,23,27,28]

A recent study suggests that disulfide formation at cysteine 42 (C42) located in the LZ domain of PKG Iα also activates PKG in a manner independent of cGMP.[29] Other work indicates oxidation-induced activation of PKG Iα mediates hydrogen peroxide-induced inhibition of intracellular calcium transient in transgenic cells[30] and dilation of human coronary arterioles.[31] C42S knock-in (KI) mice expressing mutant PKG Iα develop hypertension[32] and are resistant to the hypotensor nitroglycerin.[33] Because of the lack of response to oxidation, C42S KI mice are protected from hypotension caused by sepsis.[34]

Received: May 26, 2015
Revised: June 30, 2015
Published: July 1, 2015

DOI: 10.1021/acs.biochem.5b00572
Biochemistry 2015, 54, 4419−4422

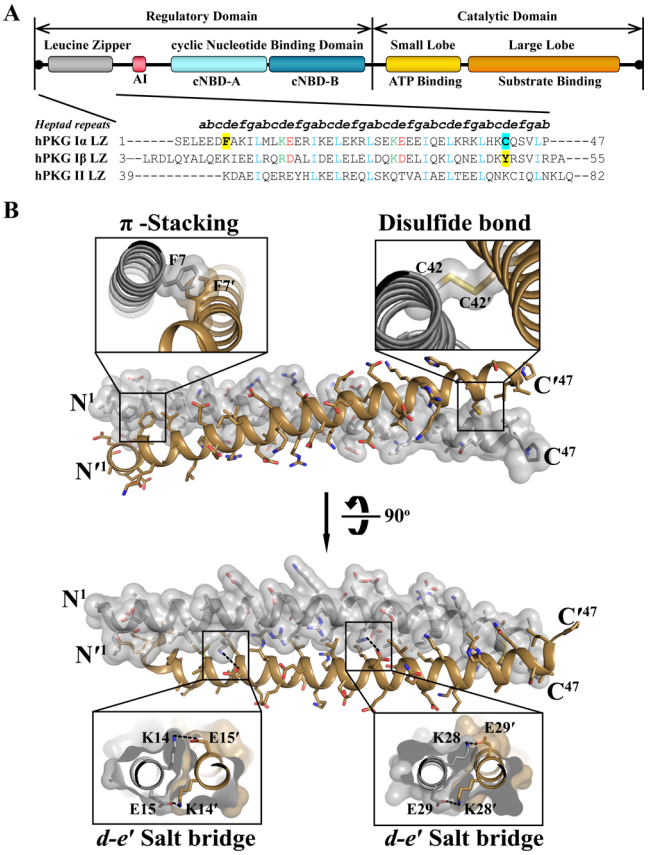

Figure 1. (A) Domain organization of PKG with the sequence of its LZ domain. AI denotes the autoinhibitory sequence. Positions within the heptad repeat are labeled *a*–*g* at the top. Hydrophobic residues at position *a* or *d* are colored blue. Basic and acidic residues forming interchain salt bridges are colored green and red, respectively. Residues involved in π-stacking are highlighted in yellow. The residue forming an interchain disulfide bond is highlighted in turquoise. (B) Overall structure of the PKG Iα LZ.

More recently, C42S KI mice were found to display a reduced neuropathic pain behavior where the mice are less sensitive to nerve injury than wild-type (WT) mice.[35] In spite of all these observations showing the physiological roles of the PKG Iα C42−C42′ disulfide bond, the molecular details of the PKG Iα LZ domain and its C42−C42′ disulfide bond remain unknown.

To gain structural insights into the C42−C42′ disulfide bond, we determined its crystal structure at 3.0 Å using a selenomethionine single-wavelength anomalous diffraction (SAD) phasing technique and further improved the resolution to 2.25 Å using native PKG Iα LZ protein (residues 1−47). The protein crystallized in hexagonal space group $P6_222$ with three molecules in the asymmetric unit (A−C). Molecules A and B form a dimer within the asymmetric unit, whereas molecule C forms a dimer with another chain C′ in the neighboring asymmetric unit (Figure S1 of the Supporting Information) [Protein Data Bank (PDB) entry 4R4L].

All three chains contain residues 1−47, showing clear electron density for the entire LZ domain used for crystallization. As predicted, they form parallel coiled-coil dimers with a dimer interface of 1281 Å^2 (Figure 1B). As expected, leucine or isoleucine residues occupy most of the "*a*" and "*d*" positions of the heptad repeat, forming the hydrophobic core. However, four non-Leu and non-Ile residues are found at the "*d*" position, also providing interhelical interactions. For example, the side chains of F7 and F7′ make a π-stacking interaction at the dimer interface, tethering the N-termini together. K14 and K28 from one monomer form an interhelical salt bridge with E15′ and E29′ from the other monomer, respectively. Finally, in the A−B dimer, C42 from one monomer forms a disulfide bond with C42′ from the other monomer, fastening the C-terminus of the LZ (Figure 1B). This bond is not present in the C−C′ dimer.

While the A−B dimer aligns well with the C−C′ dimer with an overall root-mean-square deviation of 0.981 Å, they display different *B*-factors at the C-terminus. The average *B*-factor of the C−C′ dimer at the C-terminus (residues 37−47) is 37.6 Å^2 higher than that of the A−B dimer (Figure S2A,B,E and Table S1 of the Supporting Information). Also, the unambiguous electron density around the C-terminus of the A−B dimer shows a distance of 2.03 Å between the two sulfur atoms, suggesting that both cysteine residues are fully oxidized (Figure S3A of the Supporting Information). In contrast, the C-terminal residues of the C chain show little electron density for their side chains, suggesting its C-terminus is more dynamic than the corresponding region in the A−B dimer.

PKG Iα is commonly treated with hydrogen peroxide to investigate the effect of C42−C42′ disulfide bond formation on its activity. This technique, however, suffers from adverse effects such as protein degradation and nonspecific, concentration-dependent oxidation. To overcome these effects and establish a model of constitutively oxidized LZ, we mutated C42 to leucine. We reasoned that because C42 is located at the "*d*" position of the heptad repeat, a leucine substitution would mimic the oxidized state of the LZ by facilitating the dimer interaction at the C-terminus.

The C42L PKG Iα LZ was crystallized in the same space group ($P6_222$) as the WT LZ with the same number and arrangement of chains in the asymmetric unit (PDB entry 4R4M). Its structure was determined at 1.92 Å, slightly higher than that of the WT LZ. Furthermore, both A−B and C−C′ dimers of C42L LZ display a clear electron density for all 47 residues, including the side chains of L42 (Figure S3B of the Supporting Information). Superimposing the C42L LZ with the WT LZ illustrates that the overall structure of the C42L LZ is highly similar to that of the WT LZ, including the π-stacking and interhelical salt bridges at the dimer interface. In particular, the side chains of L42 and L42′ align well with those of oxidized C42 and C42′, suggesting that the C42L mutant is structurally similar to the oxidized WT LZ (Figure S3C of the Supporting Information). While the two dimers of the WT PKG Iα LZ display different temperature factors especially in the C-terminal region, the two dimers of the C42L LZ show similar temperature factors, which are consistently lower than those of WT dimers (Figure S2C−E and Table S1 of the Supporting Information). Taken together, the C42L PKG Iα LZ is structurally analogous to the oxidized WT LZ and serves as a good model for the oxidized LZ.

Next, we investigated how disulfide formation influences the stability of the PKG Iα LZ by measuring its melting temperature (T_m) by monitoring its ellipticity at 222 nm in the absence and presence of the reducing agent β-mercaptoethanol (β-ME). To minimize the absorbance by β-ME, we optimized the concentration of β-ME to be 5 mM. In the absence of β-ME, the WT LZ showed little change in ellipticity even at the highest achievable temperature (108 °C). In the presence of 5 mM β-ME, however, it exhibited significant loss of ellipticity beginning at ∼80 °C with a T_m value of 93.0 °C (Figure S4A of the Supporting Information and Table 1). In contrast, the C42S LZ showed similar T_m values in the presence or absence of β-ME,

DOI: 10.1021/acs.biochem.5b00572
Biochemistry 2015, 54, 4419−4422

Table 1. Melting Temperatures (T_m) of PKG I Leucine Zippers Measured by Thermal Denaturation Experiments

PKG I LZ	T_m ± SEM (°C)	
	without β-ME	with β-ME
PKG Iα WT (n = 3)	>108	93.0 ± 0.8
PKG Iα C42L (n = 3)	86.3 ± 0.4	87.3 ± 0.6
PKG Iα C42S (n = 3)	81.4 ± 0.5	83.3 ± 0.7
PKG Iβ WT (n = 3)	59.3 ± 0.4	59.3 ± 0.5

which are lower than those of the WT LZ (Figure S4B of the Supporting Information and Table 1). The C42L LZ also showed similar T_m values with and without β-ME, but the values were higher than those of the C42S LZ (Figure S4C of the Supporting Information and Table 1). Lastly, the PKG Iβ LZ lacking the interchain disulfide bond showed T_m values significantly lower than those of the C42S LZ independent of the presence of β-ME (Figure S4D of the Supporting Information and Table 1).

Our structural and biophysical data demonstrate that the formation of the C42−C42′ disulfide bond stabilizes the C-terminal region of the LZ domain. Crystals of the WT LZ domain were initially obtained in the presence of a potent reducing agent, tris(2-carboxyethyl)phosphine (TCEP). However, these crystals diffracted poorly. Removing TCEP from the crystallization buffer dramatically improved the resolution limit of LZ crystals, suggesting that C42−C42′ disulfide bond formation reduces the extent of thermal motion and promotes better crystal packing. The A−B dimer shows clear electron density for the C42−C42′ disulfide bond with consistently low temperature factors throughout, while the C−C′ dimer shows weak density for the same region with higher temperature factors, indicating the formation of the C42−C42′ bond stabilizes the C-terminus of the LZ. This is further supported by the thermal denaturation experiment, in which the reduction of the interchain disulfide bond decreases the T_m of the PKG Iα LZ from >108 to 93.0 °C, which is consistent with the previously reported T_m value (94 °C).[10] Unexpectedly, the reduced WT LZ showed a T_m higher than those of C42L (87.3 °C) and C42S (83.3 °C) LZs, suggesting partial reduction under the experimental conditions used (Figure S4E of the Supporting Information).

The C42−C42′ disulfide bond is the primary contributor to the higher T_m seen in the PKG Iα LZ compared to that of the PKG Iβ LZ. Comparison of their crystal structures reveals that both LZ domains have a "*d*" position aromatic residue, which provides an interchain π-stacking interaction (F7−F7′ in Iα and Y48−Y48′ in Iβ) (Figure S5A,B of the Supporting Information), and two pairs of charged residues at positions "*d*" and "*e*", which form interchain salt bridges (K14−E15′ and K28−E29′ in Iα and R20−D21′ and K34−D35′ in Iβ). While sharing these structural features, only the PKG Iα LZ has a disulfide-forming cysteine at position "*d*" (Figure S5C of the Supporting Information).

The higher T_m of C42L and C42S Iα mutants compared to that of Iβ LZ could be explained by the different nature of the π-stacking interaction. On the basis of a study of π-stacking interaction,[36] the distance between F7 and F7′ is 3.5−4.1 Å and the two phenylalanines form a parallel stacking with slight displacement. Thus, the F7−F7′ pair falls in the stacking domain (S domain) and has an excess free energy of −6.8 kJ/mol. In contrast, the two planes of the Y48−Y48′ pair form an oblique stacking with a distance of 5.2−5.6 Å, falling into the T-shape domain (T domain). Thus, the Y48−Y48′ pair has a higher excess free energy of −6.0 kJ/mol, indicating that the Y48−Y48′ pair of Iβ is less stable than the F7−F7 pair of Iα. Hence, F7−F7′ vertical stacking might be a secondary contributor to the stability of PKG Iα.

A comparison of our X-ray structure and the nuclear magnetic resonance (NMR) ensemble of PKG Iα LZ[37] shows that the LZ assumes less compact conformations in a reducing solution (Figure S6 of the Supporting Information). Superposition of the oxidized LZ with the NMR ensemble reveals that two helices are farther apart in all states of the NMR ensemble compared to the X-ray structure. In particular, the distances between C42−C42′ side chains range between 6.1 and 11 Å in the NMR ensemble (PDB entry 1ZXA), suggesting a lack of the interchain disulfide bond.

The C-terminus of the LZ provides a docking surface for PKG Iα-specific GKAPs, and disulfide bond formation may play a role in substrate binding. A $^{1}H-^{15}N$ heteronuclear single-quantum coherence (HSQC) perturbation analysis demonstrates that residues critical for association with MYPT1 are mostly located at the C-terminus of the PKG Iα LZ, including L35, K36, K38, L39, C42, Q43, I53, and G54.[8] Pull-down assays suggest that oxidation of C42 increases the affinity of PKG Iα for RhoA by ∼10-fold.[29] Taken together, we propose that the formation of the C42−C42′ disulfide bond stabilizes the docking site for its binding partners.

Although the LZ domain is known to be crucial in mediating isotype-specific binding of PKG to its GKAPs, the molecular mechanism underlying such interactions remains under investigation. One probable explanation is the dramatic electrostatic potential difference between the three isotype-specific LZ domains. In the PKG Iα LZ, positive and negative charges are evenly distributed across the entire domain, whereas in the PKG Iβ LZ, negative charges are concentrated in the center.[38] In contrast, the PKG II LZ shows a more electroneutral surface (Figure S7 of the Supporting Information). Previous studies indicated that the Iβ LZ interacts with the transcriptional regulator TFII-I, a Iβ-specific substrate, through electrostatic interaction.[39,40] The interaction is disrupted by a high concentration of salt and abolished by mutating D25 or E30 to its counterpart in Iα, K or R, respectively. The R526E mutation of TFII-I also weakens this association, further supporting the idea that TFII-I binds the PKG Iβ LZ via electrostatic interaction.[39] Similarly, a HSQC perturbation experiment shows that K36, K38, and Q43 of the PKG Iα LZ, whose corresponding residues in PKG Iβ LZ are Q, E, and R, respectively, are among the residues most affected during its interaction with MYPT1, suggesting that electrostatic interaction mediates association between PKG Iα and MYPT1.[8] In major contrast, the crystal structure of the PKG II LZ−Rab11b complex reveals that the PKG II LZ mainly interacts with Rab11b through van de Waals interaction.[19] Taken together, the differential surface charge distribution among PKG isozymes at least partially accounts for their specificity for binding partners.

In summary, we present the first crystal structure of the PKG Iα LZ, verifying the C42−C42′ disulfide bond. The C42L LZ structurally mimics the oxidized conformation and is more stable than the C42S LZ. Thus, C42L serves as a good model for the oxidized PKG Iα LZ. Structural and biophysical analysis of WT, C42L, and C42S PKGIα LZs indicates that the formation of the interchain disulfide bond at C42 stabilizes its C-terminal region, which may facilitate its interaction with PKGIα-specific GKAPs. Our structural comparison of LZ domains of PKG Iα, Iβ, and II combined with previously reported biochemical assays suggests that the distinct distribution patterns of surface charge are important for isotype-specific GKAP interaction.

DOI: 10.1021/acs.biochem.5b00572
Biochemistry 2015, 54, 4419−4422

■ ASSOCIATED CONTENT

Supporting Information

Experimental details, supporting figures, and tables. The Supporting Information is available free of charge on the ACS Publications website at DOI: 10.1021/acs.biochem.5b00572.

■ AUTHOR INFORMATION

Corresponding Author

*E-mail: ckim@bcm.edu. Phone: 713-798-8411.

Present Addresses

[#]A.S.R.: Patheon Biologics-STL, 4766 LaGuardia Dr., St. Louis, MO 63134-3117.

[▽]E.G.: Biomedical Sciences, University of California at San Diego, La Jolla, CA 92093.

[●]M.P.Y.: School of Medicine, Texas A&M Health Science Center, Bryan, TX 77807.

Author Contributions

L.Q. and A.S.R. contributed equally to this work.

Funding

This work was funded by National Institutes of Health Grant R01 GM090161.

Notes

The authors declare no competing financial interest.

■ ACKNOWLEDGMENTS

We thank Paul Leonard (M. D. Anderson Cancer Center) for technical support in thermal denaturation experiments and Lawrence Berkeley National Laboratory for collecting the diffraction data at the Advanced Light Source.

■ REFERENCES

(1) Hofmann, F., Bernhard, D., Lukowski, R., and Weinmeister, P. (2009) *Handb. Exp. Pharmacol.*, 137−162.

(2) Francis, S. H., Busch, J. L., Corbin, J. D., and Sibley, D. (2010) *Pharmacol. Rev. 62*, 525−563.

(3) Murthy, K. S. (2006) *Annu. Rev. Physiol. 68*, 345−374.

(4) Smolenski, A. (2012) *J. Thromb. Haemostasis 10*, 167−176.

(5) Hofmann, F., Feil, R., Kleppisch, T., and Schlossmann, J. (2006) *Physiol. Rev. 86*, 1−23.

(6) Francis, S. H., and Corbin, J. D. (1994) *Annu. Rev. Physiol. 56*, 237−272.

(7) Ruth, P., Pfeifer, A., Kamm, S., Klat, P., Dostmann, W., and Hofmann, F. (1997) *J. Biol. Chem. 272*, 10522−10528.

(8) Sharma, A. K., Zhou, G. P., Kupferman, J., Surks, H. K., Christensen, E. N., Chou, J. J., Mendelsohn, M. E., and Rigby, A. C. (2008) *J. Biol. Chem. 283*, 32860−32869.

(9) Surks, H. K. (1999) *Science 286*, 1583−1587.

(10) Lee, E., Hayes, D. B., Langsetmo, K., Sundberg, E. J., and Tao, T. C. (2007) *J. Mol. Biol. 373*, 1198−1212.

(11) Tang, K. M., Wang, G. R., Lu, P., Karas, R. H., Aronovitz, M., Heximer, S. P., Kaltenbronn, K. M., Blumer, K. J., Siderovski, D. P., Zhu, Y., and Mendelsohn, M. E. (2003) *Nat. Med. 9*, 1506−1512.

(12) Michael, S. K., Surks, H. K., Wang, Y., Zhu, Y., Blanton, R., Jamnongjit, M., Aronovitz, M., Baur, W., Ohtani, K., Wilkerson, M. K., Bonev, A. D., Nelson, M. T., Karas, R. H., and Mendelsohn, M. E. (2008) *Proc. Natl. Acad. Sci. U. S. A. 105*, 6702−6707.

(13) Sanchez-Fernandez, G., Cabezudo, S., Garcia-Hoz, C., Beninca, C., Aragay, A. M., Mayor, F., Jr., and Ribas, C. (2014) *Cell. Signalling 26*, 833−848.

(14) Ammendola, A., Geiselhoringer, A., Hofmann, F., and Schlossmann, J. (2001) *J. Biol. Chem. 276*, 24153−24159.

(15) Schlossmann, J., and Densch, M. (2011) *Am. J. Physiol. Heart Circ. Physiol. 301*, H672−H682.

(16) Schlossmann, J., Ammendola, A., Ashman, K., Zong, X., Huber, A., Neubauer, G., Wang, G., Allescher, H., Korth, M., Wilm, M., Hofmann, F., and Ruth, P. (2000) *Nature 404*, 197−201.

(17) Antl, M., von Bruhl, M., Eiglsperger, C., Werner, M., Konrad, I., Kocher, T., Wilm, M., Hoffman, F., Massvergr, S., and Schlossmann, J. (2007) *Blood 109*, 552−559.

(18) Yuasa, K., Yamagami, S., Nagahama, M., and Tsuji, A. (2008) *Biochem. Biophys. Res. Commun. 374*, 522−526.

(19) Reger, A. S., Yang, M. P., Koide-Yoshida, S., Guo, E., Mehta, S., Yuasa, K., Liu, A., Casteel, D. E., and Kim, C. (2014) *J. Biol. Chem. 289*, 25393−25403.

(20) Parent, A., Hamelin, E., Germain, P., and Parent, J. L. (2009) *Biochem. J. 418*, 163−172.

(21) Taylor, S. S., Zhang, P., Steichen, J. M., Keshwani, M. M., and Kornev, A. P. (2013) *Biochim. Biophys. Acta, Proteins Proteomics 1834*, 1271−1278.

(22) Chu, D. M., Francis, S. H., Thomas, J. W., Maksymovitch, E. A., Fosler, M., and Corbin, J. D. (1998) *J. Biol. Chem. 273*, 14649−14656.

(23) Zhao, J., Trewhella, J., Corbin, J., Francis, S., Mitchell, R., Brushia, R., and Walsh, D. (1997) *J. Biol. Chem. 272*, 31929−31936.

(24) Alverdi, V., Mazon, H., Versluis, C., Hemrika, W., Esposito, G., van den Heuvel, R., Scholten, A., and Heck, A. J. (2008) *J. Mol. Biol. 375*, 1380−1393.

(25) Smith, J. A., Francis, S. H., and Corbin, J. D. (1993) *Mol. Cell. Biochem. 127-128*, 51−70.

(26) Smith, J. A., Francis, S. H., Walsh, K. A., Kumar, S., and Corbin, J. D. (1996) *J. Biol. Chem. 271*, 20756−20762.

(27) Corbin, J. D., and Doskeland, S. O. (1983) *J. Biol. Chem. 258*, 11391−11397.

(28) Wolfe, L., Francis, S., Landiss, L., and Corbin, J. (1987) *J. Biol. Chem. 262*, 16906−16913.

(29) Burgoyne, J. R., Madhani, M., Cuello, F., Charles, R. L., Brennan, J. P., Schroder, E., Browning, D. D., and Eaton, P. (2007) *Science 317*, 1393−1397.

(30) Muller, P. M., Gnugge, R., Dhayade, S., Thunemann, M., Krippeit-Drews, P., Drews, G., and Feil, R. (2012) *Free Radical Biol. Med. 53*, 1574−1583.

(31) Zhang, D. X., Borbouse, L., Gebremedhin, D., Mendoza, S. A., Zinkevich, N. S., Li, R., and Gutterman, D. D. (2012) *Circ. Res. 110*, 471−480.

(32) Prysyazhna, O., Rudyk, O., and Eaton, P. (2012) *Nat. Med. 18*, 286−290.

(33) Rudyk, O., Prysyazhna, O., Burgoyne, J. R., and Eaton, P. (2012) *Circulation 126*, 287−295.

(34) Rudyk, O., Phinikaridou, A., Prysyazhna, O., Burgoyne, J. R., Botnar, R. M., and Eaton, P. (2013) *Proc. Natl. Acad. Sci. U. S. A. 110*, 9909−9913.

(35) Lorenz, J. E., Kallenborn-Gerhardt, W., Lu, R., Syhr, K. M., Eaton, P., Geisslinger, G., and Schmidtko, A. (2014) *Antioxid. Redox Signaling 21*, 1504−1515.

(36) Marsili, S., Chelli, R., Schettino, V., and Procacci, P. (2008) *Phys. Chem. Chem. Phys. 10*, 2673−2685.

(37) Schnell, J. R., Zhou, G. P., Zweckstetter, M., Rigby, A. C., and Chou, J. J. (2005) *Protein Sci. 14*, 2421−2428.

(38) Casteel, D. E., Smith-Nguyen, E. V., Sankaran, B., Roh, S. H., Pilz, R. B., and Kim, C. (2010) *J. Biol. Chem. 285*, 32684−32688.

(39) Casteel, D. E., Boss, G. R., and Pilz, R. B. (2005) *J. Biol. Chem. 280*, 38211−38218.

(40) Casteel, D. E., Zhuang, S., Gudi, T., Tang, J., Vuica, M., Desiderio, S., and Pilz, R. B. (2002) *J. Biol. Chem. 277*, 32003−32014.

DOI: 10.1021/acs.biochem.5b00572
Biochemistry 2015, 54, 4419−4422